

VUV Testing of Science Cameras at MSFC: QE measurement of the CLASP Flight Cameras

Champey, P.^{a,b} Kobayashi, K.^b Winebarger, A.^b Cirtain, J.^b Hyde, D.^b Robertson, B.^b
Beabout, B.^b Beabout, D.^b and Stewart, M.^a

^aThe University of Alabama in Huntsville, Huntsville, AL, United States

^bNASA Marshall Space Flight Center, Huntsville, AL, United States

ABSTRACT

The NASA Marshall Space Flight Center (MSFC) has developed a science camera suitable for sub-orbital missions for observations in the UV, EUV and soft X-ray. Six cameras were built and tested for the Chromospheric Lyman-Alpha Spectro-Polarimeter (CLASP), a joint MSFC, National Astronomical Observatory of Japan (NAOJ), Instituto de Astrofísica de Canarias (IAC) and Institut D'Astrophysique Spatiale (IAS) sounding rocket mission. The CLASP camera design includes a frame-transfer e2v CCD57-10 512×512 detector, dual channel analog readout and an internally mounted cold block. At the flight CCD temperature of -20C, the CLASP cameras exceeded the low-noise performance requirements ($\leq 25 e^-$ read noise and $\leq 10 e^-/\text{sec}/\text{pixel}$ dark current), in addition to maintaining a stable gain of $\approx 2.0 e^-/\text{DN}$. The e2v CCD57-10 detectors were coated with Lumogen-E to improve quantum efficiency (QE) at the Lyman- α wavelength. A vacuum ultra-violet (VUV) monochromator and a NIST calibrated photodiode were employed to measure the QE of each camera. Three flight cameras and one engineering camera were tested in a high-vacuum chamber, which was configured to operate several tests intended to verify the QE, gain, read noise and dark current of the CCD. We present and discuss the QE measurements performed on the CLASP cameras. We also discuss the high-vacuum system outfitted for testing of UV, EUV and X-ray science cameras at MSFC.

Keywords: Characterization, Camera, CCD, VUV, Sounding Rocket

1. INTRODUCTION

The Chromospheric Lyman-Alpha Spectro-Polarimeter (CLASP) is a sounding rocket instrument that is nearing the scheduled launch date of September 3, 2015. NASA MSFC, NAOJ, IAC and IAS collaborated in the development of the CLASP instrument.

The purpose of CLASP is to measure the linear polarization profiles caused by scattering processes and the Hanle effect in the Ly- α line. The magnetic field information will be obtained from the measured Stokes Q/I and U/I profiles themselves and through detailed radiative transfer modeling of the observed Ly- α intensity and polarization using the most advanced magnetohydrodynamic models of the solar atmosphere.^{1,2} This will provide, for the first time, a diagnostic tool for magnetic field measurements in the upper chromosphere and transition region.

The CLASP instrument consists of a Cassegrain telescope optimized for reflecting the Ly- α line (121.6 nm), a slit jaw imager and the spectro-polarimeter. The spectro-polarimeter produces two spectra simultaneously (corresponding to two orthogonal polarization states). It consists of a slit, polarization modulation unit (PMU), diffraction grating, two reimaging mirrors, two polarization analyzers, and two cameras. The PMU uses a rotating 1/2 waveplate, which allows for measurement of both Stokes Q and U with fixed polarization analyzers. The rotation of the waveplate sends simultaneous trigger pulses to the cameras, which initiates frame transfer, effectively ending an exposure and beginning the next. The trigger pulses will be sent to the cameras every 300 milliseconds, and a total of 16 pulses will be sent for every rotation of the waveplate. The polarization

Further author information: (Send correspondence to Patrick Champey)

Patrick Champey: E-mail: patrick.r.champey@nasa.gov

produced by the Hanle effect in Ly- α is expected to be on the order of 0.1%.¹ Therefore the two cameras must be synchronized to a high accuracy and optimized for precision and stability.^{3,4}

Strict science requirements imposed on the CLASP cameras required a complicated design and a demanding development process. For this reason, we took advantage of the resources and facilities at MSFC and The University of Alabama in Huntsville to develop the cameras in-house. Below we discuss a series of tests performed on the CLASP flight cameras, which characterize key parameters of the camera's performance.

2. CAMERA PERFORMANCE

The science goals for CLASP called for cameras with stable, low-noise performance to accurately measure sensitive polarization signatures. The flight cameras were designed to operate with a gain of $2.0 \text{ e}^-/\text{DN}$, dark current $\leq 10 \text{ e}^-/\text{pix}/\text{sec}$, and read noise of $\leq 25 \text{ e}^-$. Meeting the low dark current requirement is achieved by cooling the detectors with liquid nitrogen (LN_2) to 253 K (-20°C). The CCD is thermally strapped to an internally mounted copper cold-block, which acts as a thermal reservoir. During the CLASP flight, the cold-block will be cooled to roughly -40°C and a heater will be used to maintain steady CCD temperature at -20°C .

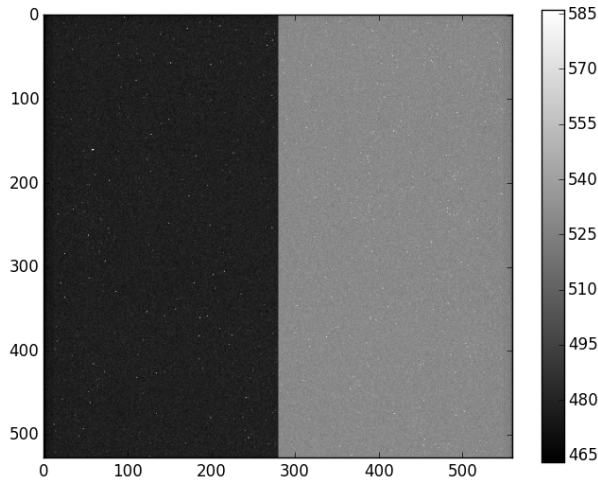


Figure 1: A typical dark frame has an offset between the left and right half. The first 280 columns are read out by the left tap and the remaining 280 columns are read out by the right tap.

The e2v CCD57-10 detectors operate in frame transfer mode. This allows for continuous exposure without the use of a shutter. The CCD57-10s are a 512×512 detector with several additional rows of inactive pixels, producing 528×560 frames. Each exposure is read out by two channels at the lowest readout rate, which optimizes for low-noise performance needed to meet science goals. Reading the CCD with two independent channels produces subtle differences in background intensity and the gain. This can be seen in a typical dark frame (Figure 1). The offset between the two halves of the detector requires measurements to be made independently for both sides.

The Solar Instrumentation lab at MSFC hosts a 245 cm L \times 60 cm D cylindrical vacuum chamber in a 10k clean room. The chamber is outfitted with an optical bench, a cryogenic flow system, vacuum translation stages, optical and thermal monitoring systems, and several UV, EUV and X-ray sources that can be interfaced to the chamber. The system is capable of achieving vacuum $< 1.0 \times 10^{-6}$ torr, via a 3-stage system of roughing, turbomolecular and cryogenic pumps. For the CLASP camera testing program, an Acton VM-502 monochromator and Hamamatsu deuterium lamp were used to generate the monochromatic Ly- α beam. A NIST calibrated Opto Diode AXUV100G photodiode and Kiethley 6485 Picoammeter were employed to measure the irradiance of the beam, which provided a standard of measurement to calibrate the camera at the Ly- α line.

Characterization of each camera was performed in vacuum, with the CCD cooled to the flight operating temperature of -20°C . Each test cycle included several data points for the measurable characteristics listed above, and typically took 8–10 hours to complete. The experiment and test procedure were configured to perform these tests in succession without having to break vacuum, or change the system.

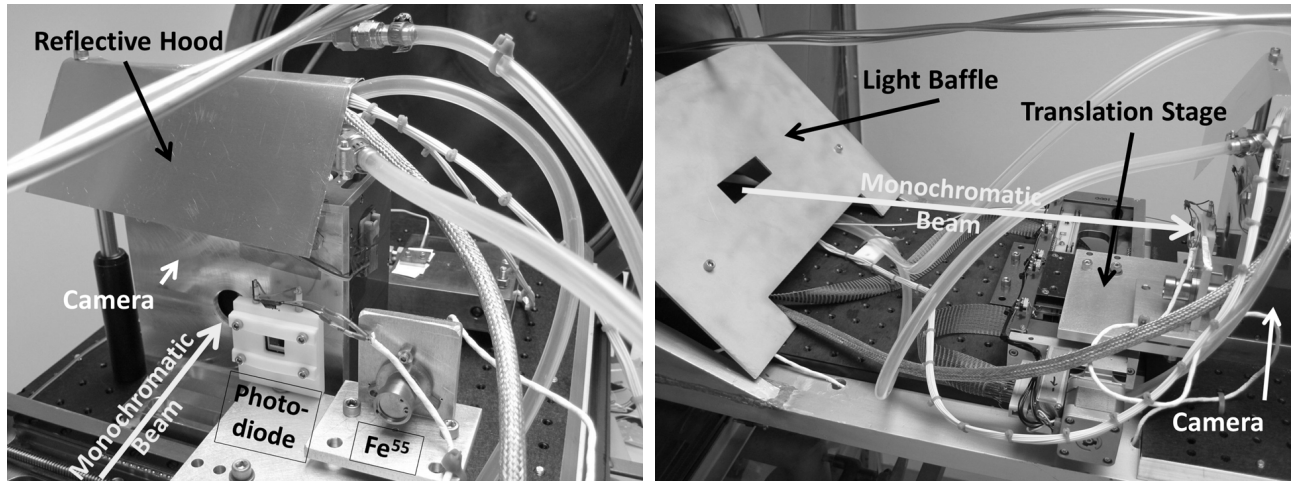


Figure 2: *Left:* Photodiode and Fe^{55} source mounted to a translation stage in front of the camera. The Fe^{55} source is used to measure the gain of the camera. *Right:* The translation stage can be seen mounted to the optics bench. A light baffle blocked the wings of the diverging beam, only passing the central Ly- α portion. The baffle was also used to test linearity. A variable intensity LED array mounted outside of a vacuum window above the chamber illuminated the baffle, creating a uniformly diffuse field.

2.1 DARK CURRENT, READ NOISE & GAIN

Dark current was measured by taking a series of dark images at different exposure times. The average dark intensity was plotted against exposure time. The slope of the line fitted to the data is the dark current rate [$\text{e}^-/\text{pix}/\text{sec}$]. Dark current measurements were performed periodically throughout each testing cycle to monitor the stability of the cameras over a long period of operation. We calculated read noise by fitting a gaussian function to a histogram of pixel intensities after dark subtraction was performed. The width of the gaussian fitted to the residual pixel intensity distribution is taken as the read noise.⁵ Results are listed in Table 1.

The camera gain is determined by the detector response to Fe^{55} photons. Fe^{55} decays into Mn, producing Mn $\text{K}_{\alpha 1}$, $\text{K}_{\alpha 2}$, $\text{K}_{\beta 1}$, and $\text{K}_{\beta 2}$ lines. These lines have well known energies and emission probabilities. We generate a histogram of the intensity of detected Fe^{55} photons and fit a quadruple gaussian function to the histogram. By determining the relative amplitudes of the 4 Mn K_{α} and K_{β} lines and the difference in intensity of the histogram peaks, the camera gain is determined.⁵⁻⁸

2.2 QUANTUM EFFICIENCY

We define the quantum efficiency of the detector as the percentage of photons that generate a signal on the detector. Taking the ratio of the number of photons detected to the number of photons incident on the detector yields the QE. e2v delivers CCDs with anti-reflective coating optimized for visible, which means high absorption in UV. In an attempt to increase the QE at the Ly- α wavelength, the CLASP e2v CCD57-10 CCDs were coated with Acton's Lumogen-E. This thin film phosphor coating absorbs UV photons then re-emits photons in the visible ($\lambda \approx 530 \text{ nm}$), a process known as fluorescence.

The quantum efficiency at Ly- α of each of the 4 cameras was measured in high-vacuum ($< 1.0 \times 10^{-6}$ torr). The cameras were mounted to an optical bench in the chamber, while the NIST calibrated photodiode was mounted to a translation stage positioned in front of the camera. The camera and photodiode were exposed to

the monochromatic Ly- α beam in alternating sets, over a period of a one hour. The photodiode would translate into the beam, record several hundred samples, then move out of the beam. This was followed by a set of camera exposures, then dark exposures for both the camera and photodiode. Multiple data points were necessary to average out any instability of the deuterium lamp. Each subset of photodiode measurements and CCD exposures were taken over a period of ≈ 1 minute: the full QE test took ≈ 1 hour to complete.

Beginning with raw FITS images, standard image reduction techniques were performed to remove dark current, fixed pattern noise and correct for gain. The average intensity over the full frame was calculated for each subset of exposures. The photodiode data was also corrected for dark current and the average number of incident photons was calculated for each subset using the NIST calibration data. Computing the ratio of the incident photons on the camera to number of photons incident on the photodiode yielded the QE. The measured QE for each of the four cameras is reported in Table 1.

Characteristic	Requirement	SN 001	SN 004	SN 005	SN 006
Gain [e^- /DN] (Left/Right)	2.0 ± 0.5	1.97/2.04	1.92/2.04	1.94/2.03	1.88/1.90
Dark Current [e^- /sec/pix] (Left/Right)	≤ 10.0	0.3/0.2	0.4/0.3	0.3/0.1	0.5/0.4
Read Noise [e^-] (Left/Right)	≤ 25.0	5.4/5.6	5.3/5.6	5.5/5.6	5.6/5.4
Quantum Efficiency [%]	30	14.2 ± 1.5	12.1 ± 1.5	20.0 ± 2.5	20.0 ± 1.9

Table 1: Summary of the performance of the three flight cameras (SN 004, SN 005, SN 006) and one engineering model/flight spare (SN 001).

In an attempt to improve accuracy in the experiment, we repeated the QE test with SN001, but with an aperture placed in the monochromatic beam. The justification for this approach was the beam uniformity was worse than expected. We placed a 5 mm diameter aperture in the optical beam to mask the photodiode and provide an equivalent area of exposure for both detectors. A correction factor of 0.8 was applied to all four cameras, which reduced the QE by 20%.

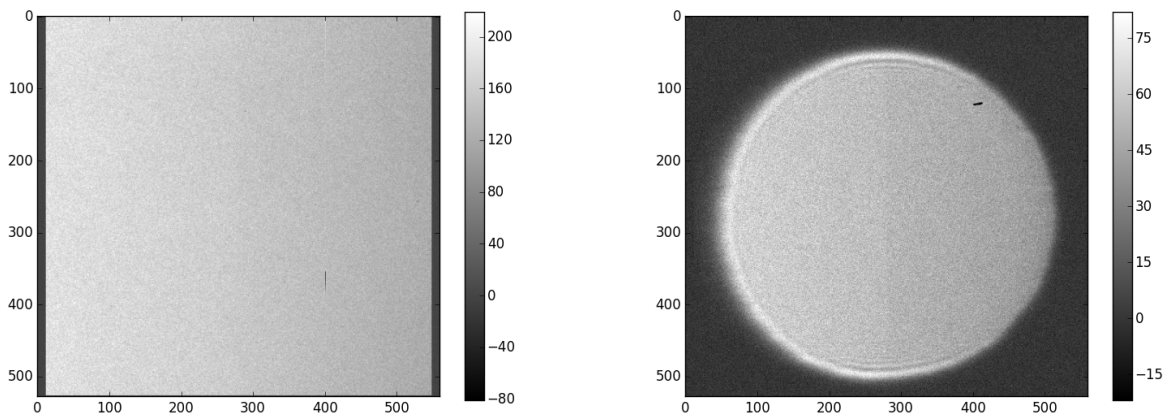


Figure 3: *Left*: A 10 second Ly- α exposure. *Right*: A 10 second Ly- α exposure after a masking the CCD.

The quantum efficiency measurements reported in Table 1 include the correction factor from masking. Cameras SN005 and SN006 were selected as the science cameras for their higher QE. SN004 was selected as the slit jaw camera. SN001 had some damage to the Lumogen-E coating, which occurred during handling of the CCD. SN001 was selected as the flight spare and was used for subsequent testing and troubleshooting.

3. CONCLUSION

The four flight cameras built for CLASP were tested in high-vacuum under flight-like conditions. The gain, dark current, read noise and quantum efficiency were measured and verified against defined requirements. The gain measured for all four cameras is within the $2.0 e^-/\text{DN}$ requirement. Some differences in gain between the readout channels were noted and a gain correction factor will be applied to science data. Measured dark current and read noise in all four cameras exceeded requirements. Dark current rate is about ≈ 30 times better than the requirement, while the readout noise is ≈ 4.5 times better than the requirement. The QE at Ly- α was measured by comparing the average number of photons detected by the CCD to the number of incident photons detected by a NIST calibrated photodiode. An aperture was installed in the monochromatic beam because the beam uniformity was worse than expected. As a result, a correction factor of 0.8 was applied to the QE measured for each camera.

ACKNOWLEDGMENTS

We acknowledge the Chromospheric Lyman-Alpha Spectro-Polarimeter grant funded by NASA's Low Cost Access to Space program under Research Opportunities in Space and Earth Sciences (ROSES). NASA MSFC led this project; partners include the NAOJ, Lockheed Martin (LMSAL), IAC, IAS, Astronomical Institute of ASCR, and the University of Oslo.

REFERENCES

- [1] J. Trujillo Bueno, J. Štěpán, and R. Casini, "The Hanle Effect of the Hydrogen Ly α Line for Probing the Magnetism of the Solar Transition Region," *ApJL* **738**, p. L11, Sep 2011.
- [2] J. Trujillo Bueno, J. Štěpán, and L. Belluzzi, "The Ly α Lines of H I and He II: A Differential Hanle Effect for Exploring the Magnetism of the Solar Transition Region," *ApJL* **746**, p. L9, Feb 2012.
- [3] R. Kano, T. Bando, N. Narukage, R. Ishikawa, S. Tsuneta, Y. Katsukawa, M. Kubo, S.-n. Ishikawa, H. Hara, T. Shimizu, Y. Suematsu, K. Ichimoto, T. Sakao, M. Goto, Y. Kato, S. Imada, K. Kobayashi, T. Holloway, A. Winebarger, J. Cirtain, B. De Pontieu, R. Casini, J. Trujillo Bueno, J. tpn, R. Manso Sainz, L. Belluzzi, A. Asensio Ramos, F. Auchre, and M. Carlsson, "Chromospheric Lyman-alpha spectro-polarimeter (CLASP)," *Proc. SPIE* **8443**, pp. 84434F–17, 2012.
- [4] K. Kobayashi, J. Cirtain, A. Winebarger, S. Savage, L. Golub, K. Korreck, S. Kuzin, R. Walsh, C. DeForest, B. DePontieu, A. Title, W. Podgorski, R. Kano, N. Narukage, and J. Trujillo-Bueno, "Sounding rocket instrument development at Univ. of Alabama in Huntsville/NASA MSFC," *Proc. SPIE* **8862**, pp. 88620P–7, 2013.
- [5] P. Champey, K. Kobayashi, A. Winebarger, J. Cirtain, D. Hyde, B. Robertson, D. Beabout, B. Beabout, and M. Stewart, "Performance characterization of UV science cameras developed for the Chromospheric Lyman-Alpha Spectro-Polarimeter (CLASP)," *Proc. SPIE* **9144**, pp. 914439–7, 2014.
- [6] J. R. Janesick, *Scientific Charge-Coupled Devices (SPIE Press Monograph Vol. PM83)*, SPIE Publications, 1 ed., 1 2001.
- [7] J. R. Janesick, *Photon Transfer (SPIE Press Monograph Vol. PM170)*, SPIE Publications, 8 2007.
- [8] I. Kotov, J. Frank, A. Kotov, P. Kubanek, P. O'Connor, M. Prouza, V. Radeka, and P. Takacs, "CCD characterization and measurements automation.," *Nuclear Instruments & Methods in Physics Research Section A-Accelerators Spectrometers Detectors and Associated Equipment* **695**, pp. 188 – 192, n.d.